Economic Synthesis and Size-Tuning of InP/ZnS and InP/ZnSe Colloidal QDs.

Mickael D. Tessier,‡* Dorian Dupont,‡ Kim De Nolf, Jonathan De Roo, Zeger Hens*

Physics and Chemistry of Nanostructures, Ghent University, Ghent, Belgium
Center for Nano and Biophotonics, Ghent University, Ghent, Belgium

Supporting Information Placeholder

ABSTRACT: We present synthesis protocols, based on indium halide and aminophosphine precusors, that allow for the economic, up-scaled production of InP Quantum Dots (QDs). The reactions attain a close to full yield conversion – with respect to the indium precursor – and we demonstrate that size tuning at full chemical yield is possible by straightforward adaptations of the reaction mixture. In addition, we present ZnS and ZnSe shell growth procedures that lead to InP/ZnS and InP/ZnSe core/shell QDs that emit from 510 nm to 630 nm with an emission linewidth between 46 nm and 63 nm. This synthetic method is an important step towards performing Cd-free QDs, and it could help the transfer of colloidal QDs from the academic field to product applications.

Colloidal QDs have rapidly evolved from a lab-scale invention of academic interest to new, useful building blocks widely applied in various fields of nanoscience and technology research.[1] This is mainly due to high precision, synthetic schemes developed for cadmium chalcogenide QDs,[2] which have made available monodisperse QD ensembles that preserve the unique, size-tunable optoelectronic properties of individual QDs. The restrictions several countries have imposed on the use of cadmium however question the long term feasibility of product applications relying on cadmium-chalcogenide based QDs, hence the quest for Cd-free alternatives.[3] This search has mainly focused on $CuInS_2$ and InP where, similar to CdSe, size quantization enables the bandgap transition to be tuned across most of the visible spectrum. Especially InP QDs combine a reduced toxicity with emission characteristics close to those of CdSe-based QDs.[4]

The strategies developed to produce colloidal InP QDs can be roughly divided in two groups. The first group includes high reactivity P(-III) precursors such as tris(trimethylsilyl)phosphine [$(TMS)_3P$][5–7] or phosphine [PH_3],[8] and the second group utilizes lower reactivity P(0) and P(+III) precursors such as trioctylphosphine (TOP),[9] P_4,[10] or PCl_3.[11] Based on size dispersion – a key parameter to be minimized for most QD-based applications – P(-III) precursors give the best results. In particular, $(TMS)_3P$ has been the most commonly used phosphorous precursor, where optimized protocols yield emission lines with a full width at half maximum (FWHM) of 40-60 nm.[12] Unfortunately, $(TMS)_3P$ is a costly and pyrophoric precursor that tends to decompose and forms lethally toxic PH_3 in contact with air. This renders upscaled $(TMS)_3P$-based InP production elusive and may explain why InP QDs are far less studied than CdSe QDs. Opposite from the high reactivity P(-III) precursors, protocols to synthesize InP QDs with low reactivity precursors yield QDs with too large a size-dispersion for most of the potential applications.

Recently, an innovative and potentially efficient alternative to make InP QDs has been published by Song *et al.*.[13] These authors use tris(dimethylamino)phosphine [$(DMA)_3P$] as a phosphorous precursor, which can be classified as a low-reactive P(+III) precursor. This compound is stable under ambient conditions and its cost is only a fraction of $(TMS)_3P$. The proposed protocol enables InP/ZnS batches to be formed, featuring emission lines with a FWHM of 60-65 nm, which is close to the best obtained with $(TMS)_3P$ (40-60 nm). Here, we take this method as a starting point to develop a InP synthesis protocol that combines economic feasibility with state-of-the art optical properties. First, we demonstrate that InP can be formed by various combinations of InX_3 (X=Cl, Br, I) and $P(amino)_3$ (amino = dimethylamino [DMA], diethylamino [DEA]) as the respective indium and phosphorous precursor. Focusing on $InCl_3$ and $(DEA)_3P$, we find that the conversion yield depends on the $(DEA)_3P:InCl_3$ molar ratio. About full yield (with respect to indium) is achieved for ratios exceeding 3.5. Moreover, replacing $InCl_3$ by $InBr_3$ or InI_3 leaves the conversion yield and the reaction rate unchanged, yet leads to InP QDs with systematically smaller diameters at the end of the reaction. Finally, we introduce ZnS and ZnSe shell growth strategies that result in InP/ZnS(e) batches with state-of-the-art emission linewidths (FWHM: 48-63 nm) and photoluminescence quantum yields (PLQY: 20-60 %). We thus conclude that $P(amino)_3$-based protocols may open a gateway to the large scale production of InP QDs.

As outlined in the Supporting Information (section S1), our first precursor for InP synthesis is a solution of $InCl_3$ and $ZnCl_2$ in a primary amine. The latter acts as both solvent and ligand and may also have a chemical role in the synthesis. Using specifically oleylamine as primary amine allows us to perform reactions at high temperatures – up to 340 °C – which is important for the eventual shell growth. In this mixture, $InCl_3$ is the actual indium precursor and $ZnCl_2$ is added to facilitate the shell growth and it also proves to reduce the size dispersion of the InP QDs. Note that, as already mentioned by other authors,[13,14] adding Zn at the beginning of the reaction does not automatically produce In(Zn)P alloys.

To form InP QDs, the $(amino)_3P$ is injected at high temperature, where we prefer tris(diethylamino)phosphine $(DEA)_3P$ because of its low price and its boiling point (240 °C) being higher than the reaction temperature (180 °C). After injection, the initially colorless reaction mixture turns dark red within ≈20 min. This is reflected in the absorption spectra of aliquots taken at different times after the injection (see Supporting Information S1).

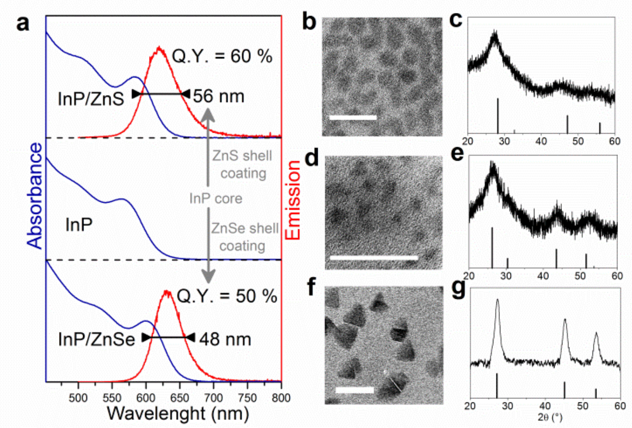

Figure 1: **a.** Overview of (blue lines) absorption and (red lines) emission spectra of InP, InP/ZnS and InP/ZnSe QDs synthesized following the reference protocols described in the Supporting Information. **b**-**g**. TEM pictures (scale bar 20 nm) and XRD diagrams of (b,c) InP/ZnS QDs, (d,e) InP QDs and (f,g) InP/ZnSe QDs.

Absorption spectra and TEM images of the InP QDs were obtained from a 20 min reaction using the reference conditions outlined in the Supporting Information (section S1) and are shown in Figure 1a and 1d. The thus formed InP QDs have an average diameter of 3.3 nm and two excitonic features, separated by ≈0.3 eV, can be distinguished in the absorption spectrum. These could correspond to transitions from the upper hole states to the first and second electron state, respectively, as this energy difference corresponds to the calculated splitting between these electron states,[ref]. Similar to InP QDs synthesized using (TMS)$_3$P, the resulting InP QDs are not luminescent, which is typically attributed to the fast oxidation of the InP surface.[15] X-ray diffraction (XRD) reveals that these InP QDs have a zinc blende structure (Figure 1e).

Around these InP cores, ZnS and ZnSe shells can be grown using the respective chalcogen precursor; sulfur or selenium dissolved in trioctlyphosphine until saturation (2.2 M), denoted as TOP-S or TOP-Se. Opposite from dodecanethiol – an alternative sulfur precursor for ZnS shell growth – we find that TOP-S does not induce a blue shift of the exciton transition upon ZnS shell growth, a phenomenon that could indicate surface etching.[13] As described in the Supporting Information, the shell growth procedure involves the addition of saturated TOP-S(e) together with zinc-stearate to the reaction mixture after the InP core formation yet before any purification. Subsequently, the temperature is increased in several steps along with additional precursor injections.

In the case of ZnS coating, the QD diameter increases to ≈6 nm (see Figure 1b), indicating that a 1.5 nm shell has been grown. In XRD, this leads to a further broadening of the diffraction peaks, probably due to the pronounced lattice mismatch between InP and ZnS (7.7%). After ZnS coating, the first exciton transition shifts to the red by ≈60 meV (Figure 1a). Moreover, photo-excitation now leads to a marked exciton emission with a linewidth of 56 nm and a PLQY of up to 60 %. These values are close to the best obtained in literature with a (TMS)$_3$P precursor and at a similar emission wavelength.[12]

The ZnSe shell growth procedure results in pyramidal QDs that are considerably larger than the InP/ZnS QDs. This enhanced growth may be linked to the smaller lattice mismatch between InP and ZnSe (3.2 %). In line with this, InP/ZnSe QDs have narrow X-ray diffraction peaks, corresponding to those of bulk ZnSe. As compared to ZnS, ZnSe coating leads to a considerable redshift (≈120 meV) of the first exciton. This can be due to its smaller band gap (2.7 eV vs. 3.6 eV for zinc blende ZnS) and its smaller conduction band offset.[16] As a result, especially the electron may be less confined in the InP core for InP/ZnSe as compared to InP/ZnS. The InP/ZnSe emission linewidth is 48 nm and the PLQY is 50 %. To the best of our knowledge, it is the first time that InP/ZnSe QDs have been synthesized with such a color-pure and efficient photoluminescence. However, the emission linewidth is still double compared to the value for CdSe QDs. This is mainly due to the worse size-dispersion as the intrinsic emission linewidth of InP and CdSe QDs are about the same.[17]

Next to precursor cost, a key element of an economical QD synthesis is the chemical yield, *i.e.*, the fraction of the precursors eventually incorporated in the QDs. Since the InP synthesis presented here is typically run using a phosphorous excess, the reaction yield is defined as the amount (moles) of indium in the InP QDs relative to the amount of indium precursor used. We calculate the yield by comparing the absorbance of quantitative aliquots at 410 nm with the intrinsic absorption coefficient of InP QDs at the same wavelength (see Supporting Information S2). Most importantly, we find that the chemical yield depends on the (amino)$_3$P:InX$_3$ ratio. Using a 1:1 (amino)$_3$P:InX$_3$ ratio, a chemical yield of 10-30 % is typically obtained. However, the yield increases to 75-85 % when the (amino)$_3$P:InX$_3$ ratio is increased to 3.6:1 or more. In this respect, it is instructive to take a look at the total synthesis cost. Counting only the cost of the chemicals, we find that in a classical (TMS)$_3$P based InP QDs synthesis, about 95 % of the total synthesis cost is due to the phosphorous precursor (see Supporting Information S3). Using (DMA)$_3$P in a 1:1 ratio to the In precursor, as proposed by Song and co-workers, reduces the synthesis cost by at least a factor of 2.5 as compared to a (TMS)$_3$P based synthesis. The increase in chemical yield with a (amino)$_3$P:InX$_3$ ratio of 3.6 further reduces this cost by a factor of 2 since the most expensive precursor – InCl$_3$ – is used more effectively. Hence, even without considering the further cost benefits of having a more stable, less hazardous precursor, it should be clear that opposite from (TMS)$_3$P, the use of (amino)$_3$P under close to full yield conditions may result in affordable InP QDs.

As QD sizes govern their optical and electronic properties, a full yield synthesis is best combined with a strategy to tune the QD size at the end of the reaction rather than stopping QD growth during the synthesis. Size-tuning at full yield has been demonstrated in syntheses for CdSe and CdS QDs by varying the reaction rate, *e.g.*, through a change of the precursor concentration.[18,19] This size-tuning strategy works with this InP QDs synthesis as well, where higher precursor concentrations indeed result in smaller QDs. However, we found that higher precursor concentrations make it harder to dissolve the solid precursors whereas decreasing the precursor concentration appears to deteriorate the size dispersion. Alternatively, size tuning at full yield and constant reaction rate proved possible with CdSe QDs, either by changing the free ligand concentration or the ligand chain length.[18,20] Keeping this result in mind, Figure 2a-c shows absorption spectra of aliquots taken during three InP QD syntheses that use different indium halides while all other reaction conditions, *i.e.*, phosphorous and zinc precursor, concentrations, solvent, solvent volume, temperature, etc., are kept constant. It follows that replacing Cl by Br and I leads to a systematic blueshift of the first exciton after a given reaction time, as shown more explicitly in Figure 2d-f. Moreover, Figures 2d-f also indicate that in all three cases the reaction rate and the eventual conversion yield (75-80%) are identical, irrespective of the halide used. In this way, the first exciton attained at the end of the reaction can be changed from 580 to 560 or 515 nm by replacing $InCl_3$ by $InBr_3$ or InI_3, respectively. We thus conclude that the InP synthesis protocols proposed here allow for an efficient size tuning at (close to) full chemical yield by a mere change of the indium halide precursor, where higher atomic number halides yield smaller QDs. To the best of our knowledge, this is the first report of size-tuning at constant reaction rate through the inorganic metal salt anion.

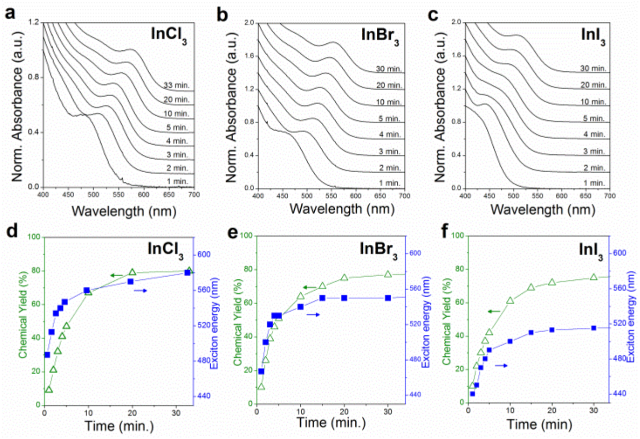

Figure 2: Development of the absorption spectrum of InP QDs using different indium precursors: **a.** InCl3 **b.** InBr3 **c.** InI3. Chemical yield and exciton energy development using different indium precursors: **d.** $InCl_3$ **e.** $InBr_3$ **f.** InI_3.

For the initially present anion to influence the outcome of a QDs synthesis, it should remain bound to the dissolved metal complex and, possibly, adsorbed at the QD surface. Although such observations have been made before for PbS QDs synthesized in oleylamine using $PbCl_2$ as a precursor,[21] it remains atypical. Indeed either Cd, Pb, Zn or In salts are most often dissolved using carboxylic or phosphonic acids as complexing agents, where the original anion is replaced by either a carboxylate or a phosphonate. In the case of indium halides and a carboxylic acid, this would result for example in the formation of either HCl, HBr or HI and indium(carboxylate)$_3$. In this case, the original anion – be it an oxide, nitrate, halide or acetate – is not expected to play a role in the synthesis.[22] Here however, InX_3 (X: halide) is dissolved in amines, which are bases that do not favor HX formation. As a result, at least part of the original anions may be retrieved in the precursor and, eventually, on the QD surface. These ideas are confirmed by the fact that the halide is detected in dried, purified InP QDs by X-ray fluorescence (see Supporting Information S4) and by the finding that replacing $ZnCl_2$ for $ZnBr_2$ or ZnI_2 has a similar effect on the QD size (see Supporting Information S5). For instance using $InCl_3$ with $ZnBr_2$ instead of $ZnCl_2$ leads to InP QDs with a first exciton at 515 nm instead of 580 nm at the end of the reaction. The smallest sizes are obtained with a mixture of InI_3 and ZnI_2. As in the case of indium halides, higher atomic number halides yield smaller sizes. Unfortunately, changing the zinc halides deteriorates the size dispersion and is therefore not seen as the most effective size tuning strategy (see Supporting Information S5).

As mentioned before, size-tuning at constant reaction rate has already been demonstrated for CdSe QDs, where it was shown to be due to a change in the moment when nucleation is stopped by growth. In this respect, increasing the free acid concentration promotes growth and thus yields larger nanocrystals through the concomitantly higher monomer solubility.[23] This explanation, however, is not satisfactorily for this InP QDs synthesis. In the case of CdSe QDs, the diameter increases and the size dispersion deteriorates with increasing monomer solubility. Here, the smallest InP QDs are obtained with InI_3, suggesting smaller solubility, yet one would expect InI_3 complexes to have a higher solubility in oleylamine than $InCl_3$ or $InBr_3$. InI_3 is less ionic and more polarizable and thus more compatible with a largely apolar coordinating solvent as oleylamine. More importantly, the smaller InP nanocrytals, synthesized using InI_3, seem to have a somewhat broader size dispersion, opposite from CdSe QDs where a dropping diameter comes with a reduced size dispersion. An alternative explanation is that in the case of the InP synthesis, QDs do not grow under diffusion control – a key assumption to link size tuning to changes in monomer solubility or diffusion coefficient. As the halides are retrieved at the InP surface, they may well affect the monomer adsorption rate, where iodides, being the most voluminous ions, will impede the monomer adsorption most. The concomitant suppression of QD growth will favor the formation of more nuclei, eventually leading to smaller QDs at the end of the reaction. On the opposite, a less voluminous halides will promote growth, lead to an earlier stopping of nucleation and thus larger QDs.

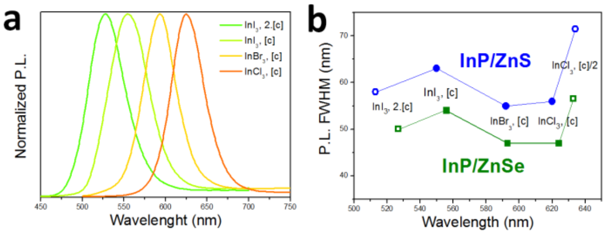

Figure 3: **a.** Emission spectra of InP/ZnSe QDs **b.** Emission linewidth of InP/ZnS and InP/ZnSe made at full chemical yield using different indium halides and different precursors concentration.

We combined the (almost) full yield size-tuning with the developed shell growth strategy to obtain luminescent InP/ZnS(e) QDs, emitting at different wavelengths. The emission spectra of different InP/ZnSe batches, shown in Figure 3a, indicate that a large part of the visible region can be addressed. In Figure 3b, the emission linewidth of several InP/ZnSe and InP/ZnS samples is plotted as a function of the emission maximum. In both cases, the three central samples (filled markers) have been synthesized by changing the indium halide precursor. This gives access to emission wavelengths between roughly 550 and 630 nm for the reference conditions used. Shorter and longer wavelength of the emission maximum can be achieved by increasing the concentration of indium iodide or reducing the concentration of indium chloride respectively (*cf.* Figure 3b, open markers). Unfortunately, a further increase of the precursor concentration is problematic due to the limited solubility of the solid precursors in oleylamine.

Figure 3b shows that ZnSe coating systematically leads to a more narrow emission than ZnS coating. Importantly, this is not due to a change in size dispersion of the initial cores, as the width of the first exciton transition is similar for each respective set of core syntheses. Possibly, this increased emission linewidth originates from the higher lattice mismatch between InP and ZnS (7.7%) than between InP and ZnSe (3.2 %). Indeed, if we measure the linewidth evolution during ZnS shell growth, we observe that the emission line progressively broadens as a function of reaction time and thus shell thickness, whereas the PLQY concomitantly increases (see Supporting Information S6). This is in line with the idea that a type 1 core/shell system is formed, where the increasing strain induced by the core/shell lattice mismatch leads to additional heterogeneous broadening. In this way, we managed to push the PLQY up to 80%, at the expense however of a larger (70 nm) linewidth (see Supporting Information S7). Opposite from this, ZnSe shell growth leads to an increase of the photoluminescence PLQY, without the increasing linewidth during shell growth. These findings underline that in the case of InP QDs, the shell growth procedure can modify the emission linewidth without changing the size dispersion of the core QDs as it has already been observed on other colloidal nanoparticles.[24] Whereas a ZnSe shell has the advantage to exhibit more narrow emission lines, we have observed that the PLQY of InP/ZnSe QDs dispersed in chloroform decreases with time. A reduction from 50 to 15% was for example measured after 6 months of storage in the dark and at room temperature. On the other hand, InP/ZnS QDs proof much more resistant to aging and their PLQY remains unchanged even after one year of storage in the same conditions This indicates that an alternate solution to combine the more narrow emission lines of ZnSe shells and the enhanced stability of ZnS shell could be to make InP/ZnSe/ZnS (see supporting information S8).

In conclusion, we have presented an economic method to make InP QDs that do not require the expensive and inconvenient $(TMS)_3P$ precursor. We use $(amino)_3P$ type precursors that allow to obtain InP QDs with a quality that is at least comparable to the best obtained in literature. We have also shown a method to size-tune the InP QDs core size at full chemical yield by playing with the inorganic moieties, linked to the metallic precursors. This full chemical yield size-tuning method combined with our shell growth procedure allows to obtain InP/ZnS and InP/ZnSe core/shell QDs with an emission that covers a large part of the visible spectrum.

ASSOCIATED CONTENT

Supporting Information

The supporting information includes the experimental part, the chemical yield evaluation, the cost estimation of the synthesis, X-Ray fluorescence measurements, InP QDs sizes obtained at full chemical yield with different zinc halides and indium halides salts, the emission linewidth evolution of InP/ZnS and InP/ZnSe QDs during a shell growth, absorption and emission spectra of InP/ZnS QDs with high PLQY. and the PLQY evolution with aging of InP/ZnS, InP/ZnSe and InP/ZnSe/ZnS QDs. This material is available free of charge via the Internet at http://pubs.acs.org.

.

AUTHOR INFORMATION

Corresponding Authors

*mickael.tessier@ugent.be
*zeger.hens@ugent.be

Present Addresses

Krijgslaan 281, building S3 (Campus Sterre), 9000 Gent, Belgium.

Author Contributions

‡These authors contributed equally.

Notes

The authors declare no competing financial interests.

ACKNOWLEDGMENT

We are grateful to K. Haustraete for TEM measurements. This work was funded by Instituut voor de Aanmoediging van Innovatie door Wetenschap en Technologie in Vlaanderen.

REFERENCES

(1) Kovalenko, M. V; Manna, L.; Cabot, A.; Hens, Z.; Talapin, D. V; Kagan, C. R.; Klimov, X. V. I.; Rogach, A. L.; Reiss, P.; Milliron, D. J.; Guyot-sionnnest, P.; Konstantatos, G.; Parak, W. J.; Hyeon, T.; Korgel, B. A.; Murray, C. B.; Heiss, W. **2015**, 1012.

(2) Murray, C. B.; Norris, D. J.; Bawendi, M. G. *J. Am. Chem. Soc.* **1993**, *115*, 8706.

(3) Anc, M. J.; Pickett, N. L.; Gresty, N. C.; Harris, J. a.; Mishra, K. C. *ECS J. Solid State Sci. Technol.* **2013**, *2*, R3071.

(4) Brunetti, V.; Chibli, H.; Fiammengo, R.; Galeone, A.; Malvindi, M. A.; Vecchio, G.; Cingolani, R.; Nadeau, J. L.; Pompa, P. P. *Nanoscale* **2013**, *5*, 307.

(5) Micic, I.; Sprague, J. R.; Curtis, C. J.; Jones, K. M.; Machol, J. L.; Nozik, A. J.; Giessen, H.; Fluegel, B.; Mohs, G.; Peyghambarian, N. *J. Phys. Chem.* **1995**, *99*, 7754.

(6) Battaglia, D.; Peng, X. *Nano Lett.* **2002**, *2*, 1027.

(7) Xie, R.; Battaglia, D.; Peng, X. *J. Am. Chem. Soc.* **2007**, *129*, 15432.

(8) Li, L.; Protière, M.; Reiss, P. *Chem. Mater.* **2008**, *20*, 2621.

(9) Lauth, J.; Strupeit, T.; Kornowski, A.; Weller, H. *Chem. Mater.* **2013**, *25*, 1377.

(10) Yan, P.; Xie, Y.; Wang, W.; Liu, F.; Qian, Y. A low-temperature route to InP nanocrystals. *Journal of Materials Chemistry*, 1999, *9*, 1831–1833.

(11) Liu, Z.; Kumbhar, A.; Xu, D.; Zhang, J.; Sun, Z.; Fang, J. *Angew. Chemie - Int. Ed.* **2008**, *47*, 3540.

(12) Li, L.; Reiss, P. *J. AM. CHEM. SOC.* **2008**, *130*, 11588.

(13) Song, W.-S.; Lee, H.-S.; Lee, J. C.; Jang, D. S.; Choi, Y.; Choi, M.; Yang, H. *J. Nanoparticle Res.* **2013**, *15*, 1750.

(14) Huang, K.; Demadrille, R.; Silly, M. G.; Sirotti, F.; Reiss, P.; Renault, O. *ACS Nano* **2010**, *4*, 4799.

(15) Jasinski, J.; Leppert, V. J.; Lam, S. T.; Gibson, G. A.; Nauka, K.; Yang, C. C.; Zhou, Z. L. *Solid State Commun.* **2007**, *141*, 624.

(16) Hinuma, Y.; Gr, A.; Kresse, G.; Oba, F. *Phys. Rev. B* **2014**, *90*, 155405.

(17) Cui, J.; Beyler, A. P.; Marshall, L. F.; Chen, O.; Harris, D. K.; Wanger, D. D.; Brokmann, X.; Bawendi, M. G. *Nat. Chem.* **2013**, *5*, 602.

(18) Abe, S.; Capek, R. K.; De Geyter, B.; Hens, Z. *ACS Nano* **2012**, *6*, 42.

(19) Owen, J. S.; Chan, E. M.; Liu, H.; Alivisatos, A. P. *J. Am. Chem. Soc.* **2010**, *132*, 18206.

(20) Abe, S.; Capek, R. K.; De Geyter, B.; Hens, Z. *ACS Nano* **2013**, *7*, 943.

(21) Moreels, I.; Justo, Y.; De Geyter, B.; Haustraete, K.; Martins, J. C.; Hens, Z. *ACS Nano* **2011**, *5*, 2004.

(22) Xu, S.; Ziegler, J.; Nann, T. Rapid synthesis of highly luminescent InP and InP/ZnS nanocrystals. *Journal of Materials Chemistry*, 2008, *18*, 2653.

(23) Flamee, S.; Cirillo, M.; Abe, S.; De Nolf, K.; Gomes, R.; Aubert, T.; Hens, Z. *Chem. Mater.* **2013**, 130528170755006.

(24) Tessier, M. D.; Mahler, B.; Nadal, B.; Heuclin, H.; Pedetti, S.; Dubertret, B. *Nano Lett.* **2013**, *13*, 3321.